Russian Journal of General Chemistry, Vol. 74, No. 8, 2004, pp. 1227–1242. Translated from Zhurnal Obshchei Khimii, Vol. 74, No. 8, 2004, pp. 1327–1342.

Mechanism of Gas-Phase Decomposition of Nitroethylene: A Theoretical Study

A. G. Shamov, E. V. Nikolaeva, and G. M. Khrapkovskii

Kazan State University of Technology, Kazan, Tatarstan, Russia

Received July 26, 2002

Abstract—Calculations by the B3LYP density functional method with various basis sets and by the QCISD(T)/6-31G(d) *ab initio* method showed that the main pathway of monomolecular gas-phase decomposition of nitroethylene is that involving a cyclic intermediate, 4*H*-1,2-oxazete 2-oxide; the barrier of its formation (201.9, 203.9, and 216.5 kJ mol^{-1}, as estimated by various methods) reasonably agrees with the experimental value (191.9 kJ mol^{-1}). The barriers of alternative pathways of gas-phase decomposition of nitroethylene are considerably higher. The barriers of reactions involving radical cations are considerably lower than those of the similar reactions involving molecules. Among all the considered pathways of nitroethylene decomposition, bimolecular pathways are the most favorable energetically.

Two major pathways of gas-phase decomposition of aliphatic nitro compounds have been proved experimentally: homolytic cleavage of the C–N bond with generation of free radicals and elimination of HNO_2 [1–4]. The molecular mechanism is realized at relatively low temperatures (up to 350°C) with mononitroalkanes containing a hydrogen atom in the α position relative to the nitro group, and also with halonitroalkanes RCH_2CHXNO_2 (X = Hlg) [2, 3]. Gas-phase decomposition of nitroethylene **I** and other α-nitroolefins is presumed to occur by a similar mechanism [2, 3, 5]. For mononitroalkanes, the molecular mechanism of HNO_2 elimination is confirmed by data on the composition of products in the initial steps of decomposition [1, 2] and by the results of quantum-chemical calculations [6–8]. Data on the composition of products formed in the initial steps of decomposition of **I** are lacking; therefore, the molecular mechanism for this compound is just a hypothesis. Published results of quantum-chemical studies of nitroethylene decomposition [9, 10] are apparently insufficient to make any definite conclusions on the primary step of the monomolecular gas-phase decomposition or to cast doubt on the suggested pathway of HNO_2 elimination. In [11, 12], we found that the barrier to elimination of HNO_2 from a molecule of **I** [223.9 kJ mol^{-1} according to B3LYP/6-311++G(df,p) calculations] significantly exceeds the experimental activation energy of the gas-phase decomposition (191.9 kJ mol^{-1}). In this work, we studied theoretically various alternative pathways of monomolecular decomposition of **I**:

$$C_2H_3NO_2 \longrightarrow C_2H_3^{\cdot} + NO_2^{\cdot}, \quad (1)$$

$$C_2H_3NO_2 \longrightarrow [\mathbf{II}]^{\neq} \longrightarrow C_2H_2 + H–O–N=O, \quad (2)$$

$$C_2H_3NO_2 \longrightarrow [\mathbf{III}]^{\neq} \longrightarrow C_2H_3–O–N=O, \quad (3)$$

$$C_2H_3NO_2 \longrightarrow [\mathbf{IV}]^{\neq} \longrightarrow CH_2=C=NO–OH, \quad (4)$$

$$C_2H_3NO_2 \longrightarrow [\mathbf{V}]^{\neq} \longrightarrow CH=CH–NO–OH^{\cdot\cdot}, \quad (5)$$

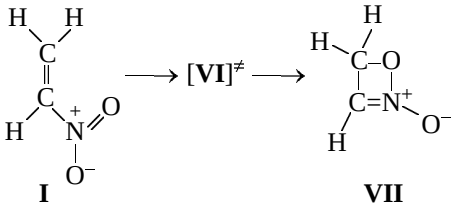

I **VII** (6)

The calculations were performed by the B3LYP/6-31G(d) and B3LYP/6-311++G(df,p) methods [13, 14]. The latter method ensures the best agreement between the experimental and calculated enthalpies of reactions and enthalpies of formation of compounds participating in monomolecular decomposition of aliphatic nitro compounds [1, 11, 12]. In some cases, the results obtained for the most important processes were checked by QCISD(T)/6-31G(d) *ab initio* calculations. The GAUSSIAN 94 and GAUSSIAN 98 program packages were used [13, 15]. Preliminary calculations were done by the PM3 semiempirical method [16]. The optimized structures of the reactants and products were used as the initial data in searching for the transition state by the algorithm of quadratic synchronous transit [17]. If this algorithm gave no result, other methods were used to determine the initial approximation for the transition state. Often the most efficient was the direct search for the transition state starting from the structure suggested by intuition. In so doing,

Table 1. Activation enthalpies of reactions (1)–(6), $\Delta H^{\neq}_{298}$, kJ mol^{-1}

Process		Compound	B3LYP		QCISD(T)/6-31G(d)
			6-31G(d)	6-311^{++}G(df,p)	
C–N bond cleavage	(1)	$C_2H_3NO_2$	281.2	268.4	289.5
		$C_2H_5NO_2$	235.9	225.6	–
HO–N=O elimination	(2)	$C_2H_3NO_2$	243.4	223.9	253.2
		$C_2H_5NO_2$	190.1	174.8	–
Nitro–nitrite rearrangement	(3)	$C_2H_3NO_2$	241.5	237.4	244.5
		$C_2H_5NO_2$	262.5	251.5	–
1,3-H shift to *aci* form	(4)	$C_2H_3NO_2$	257.6	249.2	274.8
		$C_2H_5NO_2$	281.9	271.2	–
1,4-H shift to *aci* form	(5)	$C_2H_3NO_2$	300.3	280.2	–
Cyclization	(6)	$C_2H_3NO_2$	201.3	203.9	216.5

we used, as a rule, the Baker algorithm of following the eigenvector [18].

All the extrema found on the potential energy surface were identified as minima or transition states by calculation of the vibration frequencies. To determine accurately the reagents and products in an elementary event of a chemical transformation, we made a descent along the reaction pathway from the revealed transition state in both possible directions (IRC procedure in GAUSSIAN 94 and GAUSSIAN 98).

The transition state structures calculated by the PM3 method are, as a rule, topologically equivalent to those calculated *ab initio*. However, the quantitative differences can be significant (up to 50 pm for breaking or forming bonds). Therefore, the B3LYP calculations [14] were performed in three steps. In the first step, the structure determined by PM3 calculations was used as the initial approximation for the 3-21G basis set. Then the geometry and force constants determined in the 3-21G basis set were used as the initial data for geometry optimization in the 6-31G(d) basis set, with the results being subsequently used as the initial data for 6-311^{++}G(df,p) calculations. For the extreme point determined in each basis set, we calculated force constants, vibration frequencies, and thermodynamic quantities. The descent from the transition state along the reaction pathway to the reactants and products was performed in the 3-21G and 6-31G(d) basis sets.

Some of the processes yielded singlet biradicals. For their calculation, we used the unrestricted Hartree–Fock method in which the highest occupied and lowest unoccupied molecular orbitals were mixed at the beginning of the calculations. This procedure, described in detail in [19], is equivalent to taking into account the 2×2 configuration space; it ensures correct asymptotics for dissociation processes.

The activation parameters calculated for **I** and nitroethane [reactions (1)–(6)] are listed in Table 1.

Radical decomposition. The homolytic cleavage of the C–N bond is one of the major pathways of gas-phase decomposition of nitro compounds [1–4]. The activation energy of the radical decomposition can be estimated by calculating the dissociation energy of the C–N bond, D(C–N):

$$D(\text{C–N}) = E - RT, \quad (7)$$

where E is the difference between the sum of the energies of the radicals and the energy of the initial state; R, universal gas constant; and T, temperature.

If we assume that the recombination of radicals generated by the decomposition occurs without activation barrier, then the activation enthalpy becomes equal to the enthalpy of the reaction, and D(C–N) can be determined from the enthalpies of the nitro compound and radicals:

$$D(\text{C–N}) = \Delta H^0_f(\text{R}) + \Delta H^0_f(\text{NO}_2) - \Delta H^0_f(\text{R–NO}_2). \quad (8)$$

In quantum-chemical calculations, D(C–N) is usually determined from the total electron energies. However, we also calculated the enthalpies (at 0 and 298.15 K) with the aim to evaluate the temperature dependence of the dissociation energy of the C–N bond. Also, the use of enthalpies allows in some cases their comparison with available thermochemical data, to assess the reliability of the values obtained.

The validity of Eq. (8) for gas-phase decomposition of nitroalkanes is substantiated in [20, 21]. It is noted

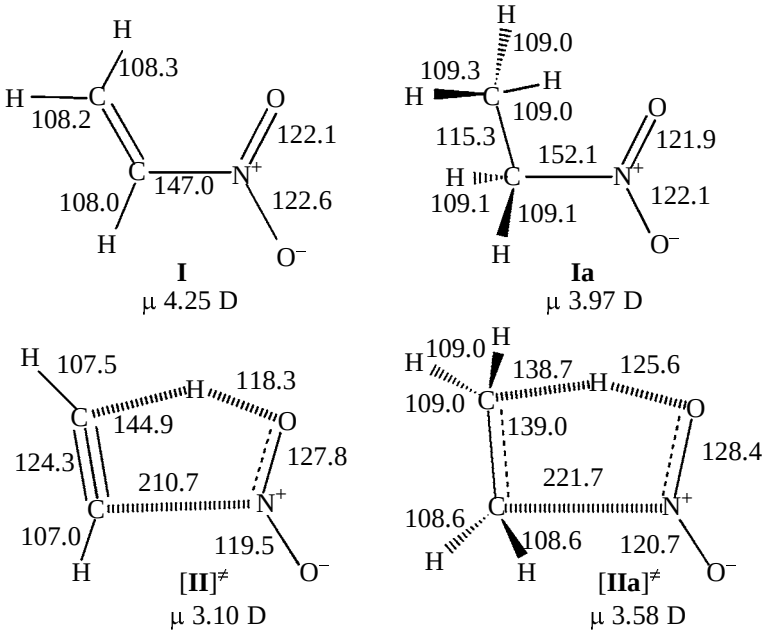

Fig. 1. Geometric parameters and dipole moments of the reactants (nitroethylene **I** and nitroethane **Ia**) and transition states of HNO_2 elimination (from nitroethylene, [**II**]$^{\neq}$; from nitroethane, [**IIa**]$^{\neq}$), according to B3LYP/6-311^{++}G(df,p) calculation (bond lengths in pm).

that, in radical decomposition of nitromethane, nitroethylene, and some halonitromethanes, the reverse reaction has no barrier. If the barrier exists, then Eq. (8) gives the lower estimate for *D*(C–N). Obviously, elucidation of whether the barrier exists is of interest in cases when the radical pathway is the major pathway of monomolecular decomposition. However, the calculated activation enthalpy of radical detachment of the NO_2 group from nitroethylene is considerably (by 84 kJ mol^{-1}) higher than the experimental activation energy. Possible errors in B3LYP calculations with the basis sets used do not exceed 13–17 kJ mol^{-1} [7, 20]. Therefore, at temperatures of the experimental studies (280–320°C [1]), the contribution of the radical pathway to the apparent activation energy will be negligible. Therefore, we did not specially study how the enthalpy of **I** varies with stretching of the C–N bond, which would reveal a barrier, if any, to recombination of the radicals.

Note that *D*(C–N) in nitroethylene is higher than that in nitroethane by 45.3 kJ mol^{-1} [B3LYP/6-31G(d)]. Although calculations with the 6-31G(d) and 6-311^{++}G(df,p) basis sets give different *D*(C–N) values (by ~12.5 kJ mol^{-1}), the above difference between nitroethylene and nitroethane is preserved. It should be noted that the *D*(C–N) values estimated by the B3LYP/6-31G(d) method [20, 21] for nitromethane, nitroethane, and isomeric nitropropanes coincide within 4–8 kJ mol^{-1} with the experimental activation energies of gas-phase decomposition of these compounds. Therefore, we believe that the estimated values of *D*(C–N) and activation enthalpy of radical decomposition of **I** are also sufficiently reliable.

Elimination of HNO_2. We have already noted that the results of experimental studies are discussed in terms of this mechanism. In so doing, however, certain questions arise.

First, it is difficult to explain within the framework of a common mechanism why the activation energies for compounds with essentially different geometric and electronic structures, nitroethane and nitroethylene, coincide. One of the reaction products, HNO_2, is the same in both cases. Elimination of HNO_2 via a five-membered transition state involves significant variation of the C–N bond length [22], and, as shown above, the *D*(C–N) values for nitroethane and nitroethylene differ considerably. Furthermore, it is quite obvious that the energy gain in formation of a double bond in decomposition of nitroethane to ethylene substantially exceeds the energy gain in formation of a triple bond in decomposition of **I** to acetylene. Therefore, it could be expected that the activation energy (enthalpy) of decomposition of nitroethylene would be appreciably higher compared to nitroethane.

Figure 1 shows the geometric parameters of compound **I**, nitroethane **Ia**, and transition state of the cor-

responding reactions of HNO_2 elimination. The results of *ab initio* calculation also suggest that the barrier to elimination of HNO_2 from nitroethylene is higher compared to nitroethane. Appreciable (up to 33.5–50.2 kJ mol^{-1} depending on the basis set) differences between nitroethylene and nitroethane in the activation energy of HNO_2 elimination exceed the possible error of estimation of the reaction barrier. Therefore, the calculation results do not confirm the conclusion made in experimental studies [1, 2] that the gas-phase decomposition of **I** follows the pathway of HNO_2 elimination.

Analysis of the geometry of the transition state in the reactions of nitroethane, [**IIa**]$^{\neq}$, and nitroethylene, [**II**]$^{\neq}$, shows that the bond angles in the five-membered rings in these structures are very close. At the same time, the angles at the CH_2 and CH groups in the transition state differ essentially. In the reaction of **I**, an acetylene structure is formed, and the corresponding angles (141° and 167.5°) strongly differ from those observed in the starting molecule (120.3° and 120.7°). Such changes involve large energy consumption. In the reaction of nitroethane, the bond angles at the CH_2 group change to a lesser extent. The C–NO_2 bond lengths in the transition states of the reactions of nitroethylene and nitroethane are fairly close, whereas the C–C bond is noticeably longer in [**IIa**]$^{\neq}$.

From the viewpoint of comparison of the activation enthalpies of the two processes, it is important to compare changes in the geometric parameters in going from the starting molecules to the transition states.

Calculations show that the largest difference is observed in variation of the C–H bond length. In the reaction of nitroethylene, Δr(C–H) is more than 10 pm larger compared to nitroethane. Furthermore, calculation suggests that the arising O–H bond in [**II**]$^{\neq}$ is appreciably shorter than in [**IIa**]$^{\neq}$, which should also increase the activation barrier. Changes in the lengths of the other valence bonds in the reactions of **I** and nitroethane are similar. In going from the starting molecule to the transition state, the C=C bond length in nitroethylene changes to a somewhat lesser extent compared to the related bond length in nitroethane. It should be noted, however, that the double bond in **I** is appreciably stronger than the related single bond in **Ia**. Therefore, presumably, changes in the C–C bond lengths make similar contribution to the reaction barrier in the cases of nitroethylene and nitroethane.

The substituent effect on the activation energy of gas-phase elimination of HNO_2 from aliphatic nitro compounds is discussed in experimental studies using the concept of a polar transition state [2, 21]. Quantum-chemical calculations, however, do not support this assumption (Fig. 1). The dipole moments of the starting nitroethane and nitroethylene molecules are higher than those of the corresponding transition states. Therefore, the conclusions of the Maccol–Benson theory developed for additions and eliminations via a four-membered transition state (which is, indeed, more polar than the starting molecules, according to the calculations [4]) cannot be applied to β-elimination of HNO_2 via a five-membered transition state.

Thus, the calculation results do not confirm the conclusion made in [2, 3] that gas-phase decomposition of nitroethylene follows the pathway of HNO_2 elimination. This is indicated by not only B3LYP but also QCISD(T) calculations.

Nitro–nitrite rearrangement. The nitro–nitrite rearrangement has been extensively studied [21, 23–25]; the most detailed data were obtained for nitromethane and nitrobenzene. The main conclusion following from the ab initio studies is that the activation enthalpy of the nitro–nitrite rearrangement in nitroalkanes is considerably higher than D(C–N). Since the radical pathway is characterized by considerably higher preexponential term, the occurrence of the nitro–nitrite rearrangement is improbable. With nitrobenzene and its derivatives, the pattern is somewhat different. According to MP2/6-31G(d)//3-21G calculations, the barrier to nitro–nitrite rearrangement in nitrobenzene is more than 41.8 kJ mol^{-1} lower than D(C–N), and at relatively low temperatures this pathway can make a significant contribution to the overall process along with radical decomposition [24]. Similar conclusion follows from the results of a B3LYP/6-31G(d) study of nitro–nitrite rearrangement in a large series of aromatic nitro compounds [25].

In this connection, the specific features of the nitro–nitrite rearrangement of **I** are of considerable interest. As seen from Table 1, the barriers predicted by B3LYP/6-31G(d), B3LYP/6-311^{++}G(df,p), and QCISD(T)/6-31G(d) calculations differ by no more than 7 kJ mol^{-1}. The activation enthalpies of the reactions of nitroethylene and nitrobenzene [4] also differ insignificantly, being appreciabaly lower than D(C–N). As already noted, the calculated D(C–N) values for nitrobenzene and **I** are also similar. The barrier to the nitro–nitrite rearrangement in nitroethane is more than 21 kJ mol^{-1} higher than in nitroethylene. The geometric parameters of the reactions, given in Table 2, explain this difference. The C–N and N–O bond lengths change most significantly in the transition state of the nitro–nitrite rearrangement, compared to the starting molecules. For the reaction involving

nitroethane, Δr(C–N) is considerably larger compared to **I** (51.4 and 16.5 pm, respectively), which results in higher activation enthalpy. The calculated barrier to the nitro–nitrite rearrangement in nitroethane is 46–50 kJ mol^{-1} higher (depending on basis set) than the experimental activation energy of gas-phase decomposition of nitroethylene. Since the *A* factor of the reaction, as tentatively estimated from the activation free energy, is within $10^{12.5}$–10^{13} s^{-1}, this process cannot be major in gas-phase decomposition of **I**.

It is also interesting to consider the secondary process of radical decomposition of vinyl nitrite:

$$CH_2CHONO \longrightarrow CH_2CHO^* + NO^*. \qquad (9)$$

Thermodynamic estimation of the barrier of reaction (9) by the B3LYP/6-31G(d) method, assuming that the reverse radical recombination occurs without a barrier, gives a very low value, 55.7 kJ mol^{-1}. Unfortunately, we found no experimental data on *D*(O–NO) of vinyl nitrite. However, the known dissociation energies of the O–NO bond in some aliphatic nitrites, e.g., in methyl nitrite (152.3 kJ mol^{-1}) and ethyl nitrite (143.5 kJ mol^{-1}) [26], exceed this value by a factor of almost 3. To make these data consistent, we have to assume the existence of a barrier to the reverse reaction. In this connection, we studied in detail the curve of energy variation in stretching of the O–NO bond in vinyl nitrite. We revealed a transition state; a descent from it leads either to vinyl nitrite or to its isomer, CH_2NO–C(H)=O (Fig. 3), lying lower in energy than vinyl nitrite by 39.9 kJ mol^{-1}. The barrier of this reaction is 51.6 [B3LYP/6-31G(d)] or 55.6 kJ mol^{-1} [QCISD(T)].

Formation of *aci*-nitroethylenes. Recent studies of formation of aci forms of nitroalkanes gave new important results. As noted in [7, 23, 24], studies of *aci*-nitro compounds are of interest for understanding the causes of abnormally low stability of dinitromethane and the mechanism of liquid-phase decomposition of nitro compounds. For nitroethylene, we considered

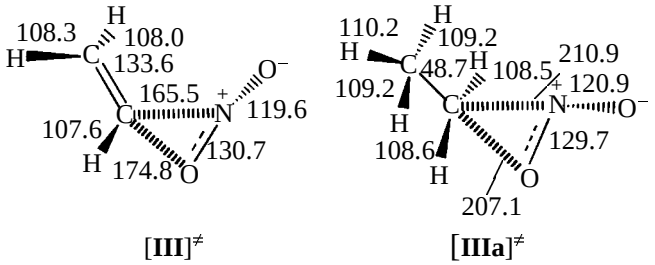

Fig. 2. Geometric parameters of the transition states (from nitroethylene, [**III**]$^{\neq}$; from nitroethane, [**IIIa**]$^{\neq}$) of the nitro–nitrite rearrangement, calculated by the B3LYP/6-311^{++}G(df,p) method (bond lengths in pm).

two alternative processes of formation of *aci* forms, involving 1,4- and 1,3-sigmatropic shift, respectively. The latter process is biradical, and the transition states of these reactions are essentially different (Fig. 4).

The barrier to 1,3-H shift to the *aci* form (Table 1) is considerably higher than that in nitroalkanes; the calculations indicate that this mechanism cannot noticeably contribute to the gas-phase decomposition of nitroethylene. In contrast to nitroethane, in nitroethylene one more route to the *aci* form is possible: 1,4-H shift. For nitroalkanes, the corresponding reactions yielding unstable cyclic products are energetically unfavorable a fortiori; therefore, we did not study the similar process with nitroethane. The pattern may change owing to the presence of a double bond and a common conjugated system in **I**. The geometries of the transitions states of the 1,3-sigmatropic hydrogen shift in nitroethane and nitroethylene and of the 1,4-H shift in **I**, calculated by the B3LYP/6-311^{++}G(df,p) method, are compared in Fig. 4. It is seen that, for the 1,3-H shift, the calculated geometric changes in nitroethylene in going from the starting molecule to the transition state are considerably smaller compared to nitroethane. For example, the C–N bond length in the transition state of the reaction of **I** remains virtually unchanged, and the N–O and C–H bonds change to a

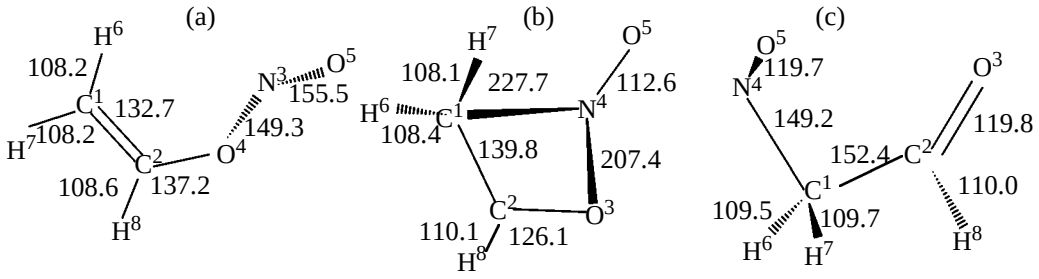

Fig. 3. Geometric parameters of (a) vinyl nitrite, (b) transition state, and (c) isomerization product (nitrosoacetaldehyde), calculated by the B3LYP/6-311^{++}G(df,p) method (bond lengths in pm).

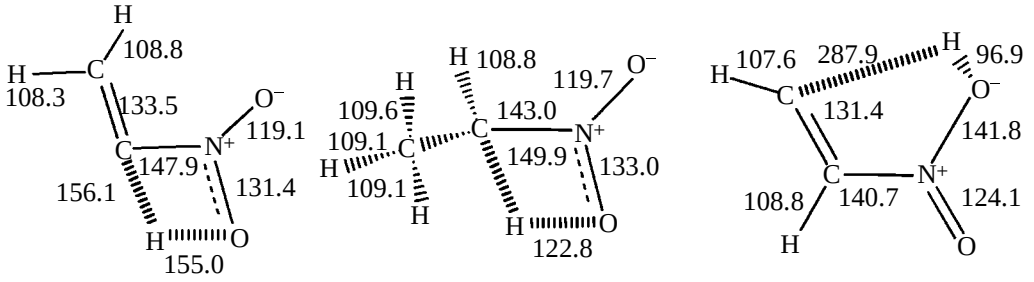

Fig. 4. Geometric parameters of the transition states of 1,3-sigmatropic hydrogen shift in nitroethylene ([**IV**]$^{\neq}$) and nitroethane ([**IVa**]$^{\neq}$) and of 1,4-H shift in nitroethylene ([**V**]$^{\neq}$), calculated by the B3LYP/6-311^{++}G(df,p) method (bond lengths in pm).

lesser extent; this accounts for the fact that the activation enthalpy of the reaction of **I** is almost 23 kJ mol^{-1} lower compared to nitroethane. The 1,4-H shift is considerably less favorable energetically, as it occurs via a five-membered biradical transition state, with significant changes in the lengths of three bonds: C–C, C–N, and N–O. As compared to the 1,3-H shift, the N–O bond length increases by almost 10 pm, and the C–N bond length, by 7 pm. These changes involve larger energy consumption than stretching of the C–N bond (in the case of 1,3-sigmatropic shift). Therefore, the barrier of this reaction noticeably exceeds the activation enthalpy of the 1,3-sigmatropic shift in nitroethylene [27].

Thus, our results show that the barriers to formation of the aci forms are so high that these processes cannot significantly contribute to the gas-phase monomolecular decomposition.

New mechanism of nitroethylene decomposition. The activation enthalpies of all the above-considered reactions considerably exceed the experimental activation energy of gas-phase decomposition of **I**. Therefore, we studied an alternative process (6) involving formation of a cylcic product, 4*H*-1,2-oxazete 2-oxide **VII**.

This pathway was suggested for the first time by Kinstle and Stam [28] as applied to high-temperature pyrolysis of β-nitrostyrenes:

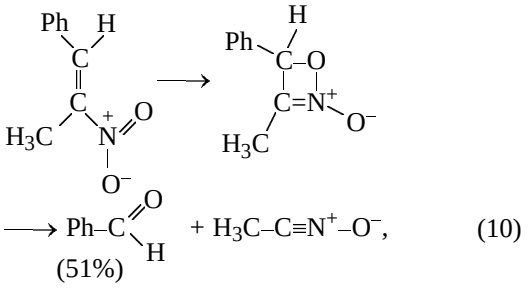

$$+ H_3C–C\equiv N^+–O^-, \qquad (10)$$

$$H_3C–C\equiv N^+–O^- \longrightarrow \begin{cases} H_3C–C\equiv N\ (25\%) + O, \\ H_3C–N=C=O\ (15\%). \end{cases} \qquad (11)$$

The major products of reactions (10) and (11) are PhCHO and CH_3CN, which suggested such a pathway. However, it was not confirmed in [28] by any kinetic or energy data.

Although formation of **VII** in thermal decomposition of nitroethylene was not proved experimentally, related oxazetes were prepared by cyclization of substituted nitroethylenes [29, 30].

The result furnished by an *ab initio* study was, at first glance, unexpected. According to B3LYP calculations, reaction (6) is the most favorable pathway of monomolecular decomposition of nitroethylene, and its calculated barrier is close to the experimental activation energy. The difference, ~8 kJ mol^{-1}, is within the possible error of the experimental determination. On the other hand, an 8–12 kJ mol^{-1} error is also possible in calculation of the activation enthalpy; thus, the agreement between the calculated and experimental reaction barriers is quite reasonable. It is important that 6-31G(d), 6-311^{++}G(df,p), and QCISD(T)/6-31G(d) calculations give very close activation enthalpies of the reaction [31], which also confirms the reliability of the calculation results.

The considerably lower barrier of reaction (6), compared to that of the competing reaction (2), may be accounted for by the fact that in the four-membered transition state, in contrast to the five-membered transition state of HNO_2 elimination, only three valence bonds (and not four, as in monomolecular decomposition of nitroalkanes) significantly change. However, it is more important to analyze these changes quantitatively. When discussing β-elimination of HNO_2 from **I**, we already noted that the most significant changes, compared to the starting molecules, occur with the

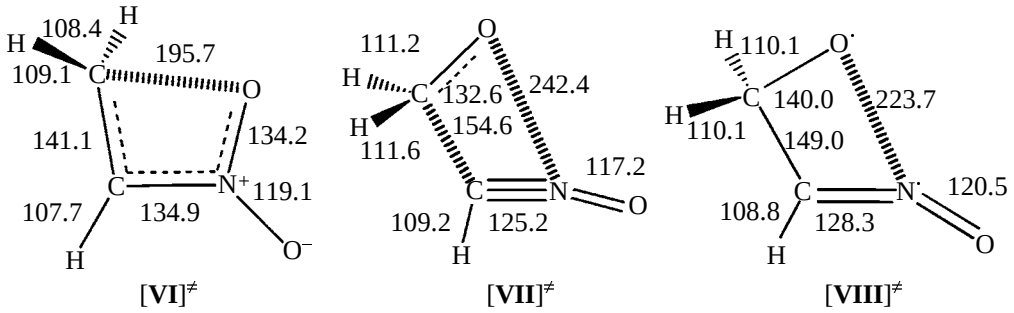

Fig. 5. Geometric parameters of the transition states of formation of 4*H*-1,2-oxazete 2-oxide **VII** ([**VI**]$^{\neq}$), concerted one-step decomposition of **VII** ([**VII**]$^{\neq}$), and primary step in the multistep pathway of decomposition of **VII** ([**VIII**]$^{\neq}$), calculated by the B3LYP/6-311^{++}G(df,p) method (bond lengths in pm).

C–N and C–H bonds. At the same time, in the transition state of reaction (6), the C–H bond remains virtually unchanged, and Δr(C–N) is 55 pm smaller compared to elimination of HNO_2. Calculation shows that Δr(N–O) and Δr(C–C) in formation of the cyclic intermediate [reaction (6)] are somewhat larger (by 50 and 10 pm, respectively), compared to elimination of HNO_2. However, it is quite clear that, on the whole, the structure of the transition state of reaction (6) is considerably closer to nitroethylene, which accounts for the lower barrier (Figs. 1, 5).

To assess the feasibility of the suggested pathway, it is important to examine its subsequent steps. As a similar scheme [Eqs. (10), (11)] was suggested to account for formation of the experimentally detected products in pyrolysis of nitrostyrenes, it is natural to expect formation of related products (in particular, formaldehyde and hydrogen cyanide) in gas-phase decomposition of nitroethylene.

The results of studying secondary processes of decomposition of 4*H*-1,2-oxazete 2-oxide are summarized in Scheme 1 [results of B3LYP/6-311^{++}G(df,p) calculations]. The figures in parentheses below the arrows are reaction numbers, and the figures above the arrows are the relative enthalpies of formation of the transition states of the given reactions (kJ mol^{-1}); the enthalpy of formation of nitroethylene is taken as zero.

Scheme 1.

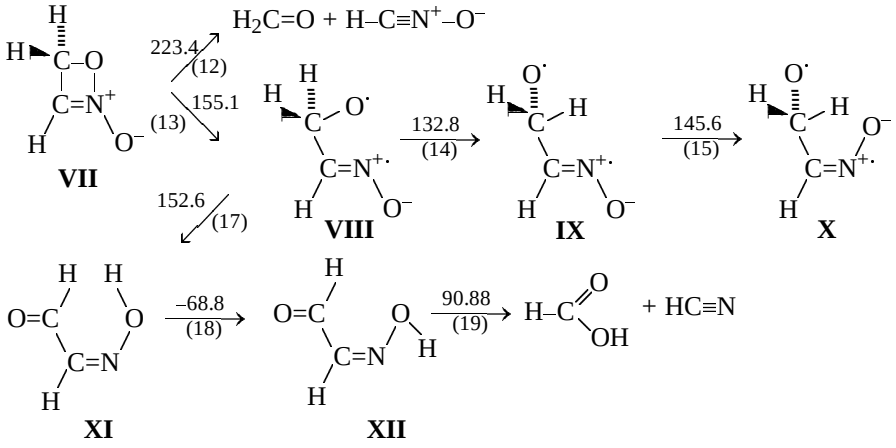

Concerted pathway (12) directly yielding the reaction products, formaldehyde and nitrile oxide, has the barrier exceeding the experimental activation energy of decomposition of **I** and the calculated activation enthalpy of primary reaction (6); hence, it cannot be the major pathway of pyrolysis. An alternative pathway involves formation of a singlet biradical intermediate **VIII** [reaction (13)], which decomposes into

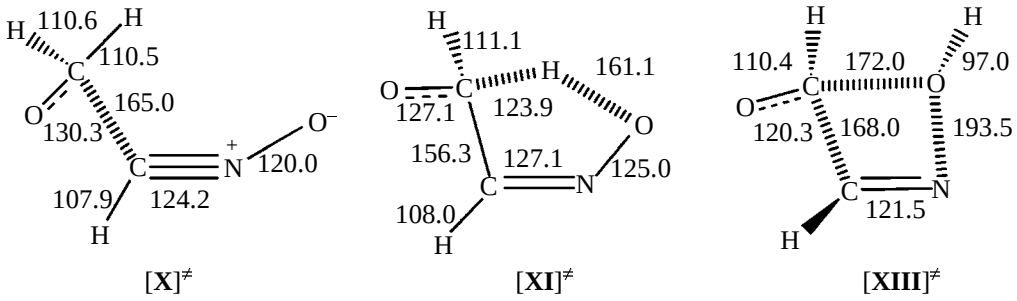

Fig. 6. Geometric parameters of the transition states of secondary processes of nitroethylene decomposition: [**X**]$^{\neq}$ [process (16)], [**XI**]$^{\neq}$ [process (17)], and [**XIII**]$^{\neq}$ [process (19)], calculated by the B3LYP/6-311^{++}G(df,p) method (bond lengths in pm).

formaldehyde and nitrile oxide [reaction (16)] after a series of conformational transitions (14) and (15). The geometric parameters of the structure of the transition state [**X**]$^{\neq}$ of reaction (16) are given in Fig. 6.

Intermediate **VIII** is formed in reaction (13) with cis conformation of the O–C–C–N group. Analysis of the charge distribution on the oxygen atom and NO group in **VIII** shows that this group is not a zwitter ion (in particular, the charge on the O atom decreases by 0.1 e, and that on the NO group increases by the same value as compared to **VII**). On the contrary, the spin density in **VIII** is strongly polarized (–0.83 *e* on the O atom and 1.0 *e* on the NO group).

Process (14) is rotation around the C–C bond by 130°. The transition state corresponds to the rotation angle of 54°. The second transition state corresponds to the trans orientation of the O–C–C–N group (rotation by 180°); it separates two equivalent gauche conformations differing only in the rotation direction.

Step (15) is rocking motion of the N–O bond in the C–C–N–O plane. In the transition state, the C–N–O fragment is approximately linear.

Another pathway of decomposition of biradical **VIII** is its rearrangement (17) into aldoxime **XI**, which after conformational transition (18) involving rotation of the OH group around the NO bond decomposes into hydrogen cyanide and formic acid [reaction (19)]. The geometric parameters of transition states [**XI**]$^{\neq}$ and [**XIII**]$^{\neq}$ of processes (17) and (19) are shown in Fig. 6.

These two decomposition pathways are virtually equivalent energetically. As already noted, aldehydes and nitriles were detected as major products of pyrolysis of β-nitrostyrenes [28].

Although we have not considered some other pathways (e.g., those yielding cyclic peroxides), this will not alter the main conclusion: The revealed secondary processes of decomposition of cyclic intermediate **VII** have considerably lower activation enthalpies than the experimentally measured activation energy of the primary step of gas-phase decomposition of **I**, and these processes yield products that were detected experimentally in pyrolysis of nitroolefins. Thus, the calculations show that formation of 4*H*-1,2-oxazete 2-oxide is the primary limiting step of nitroethylene decomposition. The barriers of all the other alternative processes are higher, which is also confirmed by ab initio estimations [32].

The only energetically feasible decomposition pathway of **VII** is formation of singlet biradical **VIII**. The diversity of possible subsequent transformations is provided by the large number of conformations of **VIII**.

Possible objections that decomposition of 4*H*-1,2-oxazete 2-oxide yields a zwitterion rather than biradical are refuted by data on distribution of charges and spin densities, and also by dipole moments of the corresponding structures. These data unambiguously show high degree of polarization of the spin density on the oxygen atom and NO group of biradical **VIII** and insignificant charge redistribution relative to the starting structure **VII** (Fig. 7, Table 2). For the structure CH=CH–N˙O–OH, the results are similar.

Thus, the new mechanism of decomposition of **I**, with reaction (6) as the primary step, is the most favorable energetically among all the alternatives. The activation energy of this process reasonably agrees with the experimental activation energy of the gas-phase decomposition. Furthermore, the theoretical study confirmed the possibility of formation of formaldehyde and hydrogen cyanide. As already noted, the related products were detected in gas-phase pyrolysis of nitrostyrenes decomposing, apparently, by the similar mechanism.

To conclude, we should note certain important features of the mechanism under consideration. First, in contrast to HNO_2 elimination, it is specific for

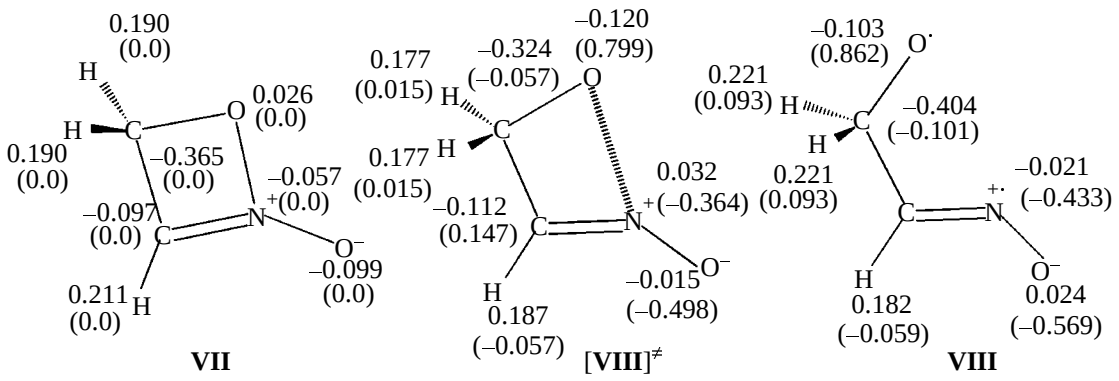

Fig. 7. Charges (in parentheses, spin densities) on atoms of 4*H*-1,2-oxazete 2-oxide **VII** and of transition state [**VIII**]$^{\neq}$ and product **VIII** of reaction (13), calculated by the B3LYP/6-311^{++}G(df,p) method.

compounds containing an NO_2 group in the α-position to the carbon atom forming the double bond. Also, the reaction is multistep, whereas elimination of HNO_2 directly yields the reaction product.

Finally, the most significant feature of the suggested mechanism is participation of biradical transition state and biradical reaction products. Previously such reactions were not considered when discussing gas-phase decomposition of nitroolefins and other C-nitro compounds at relatively low temperatures.

Decomposition of nitroethylene radical cation. Formation of cyclic intermediate **VII** in decomposition of nitroethylene is confirmed by the mass spectra [33]. However, the mass-spectrometric data cannot be straightly applied to transformations of molecular nitroethylene, since they concern fragmentation of radical cations rather than decomposition of molecules. The barriers of reactions involving radical cations can significantly differ from those of similar processes involving neutral molecules. For example, the mass spectrum of products of high-vacuum pyrolysis of nitromethane, recorded in the field ionization mode, contains an NO^+ peak (*m/z* 30). This peak was considered as an evidence that the primary step of the pyrolysis is nitro–nitrite rearrangement [4]. However, the results of semiempirical (PM3), ab initio (QCISD, CASSCF, MP2, MP4), and density functional (B3LYP) calculations show that the barrier of nitro–nitrite rearrangement exceeds the dissociation energy of the C–N bond, which excludes realization of this mechanism in the gas phase [25]. Reliable theoretical estimates of the barriers of reactions involving radical cations of **I** are lacking; therefore, we examined in this work the main alternative processes. Localization of the critical points on the potential energy surface and descents along the reaction pathway from the transition state to the reactants and products were performed with the B3LYP/6-31G(d) method. Note that we do not consider the features of formation of the radical cations and do not discuss the mass spectra of nitroethylene and its decomposition products. This is a complex and specific problem requiring a separate detailed study.

As for the neutral molecule of **I** [31], we examined six major pathways (20)–(25) of monomolecular decomposition of its radical cation:

$$C_2H_3NO_2\rceil^{+\cdot} \longrightarrow C_2H_3\rceil^{+} + NO\rceil\cdot, \quad (20)$$

$$C_2H_3NO_2\rceil^{+\cdot} \longrightarrow [\mathbf{IIc}]^{\neq} \longrightarrow C_2H_2 + H\text{–}O\text{–}N{=}O\rceil^{+\cdot}, \quad (21)$$

$$C_2H_3NO_2\rceil^{+\cdot} \longrightarrow [\mathbf{IIIc}]^{\neq} \longrightarrow C_2H_3\text{–}O\text{–}N{=}O\rceil^{+\cdot}, \quad (22)$$

$$C_2H_3NO_2\rceil^{+\cdot} \rightarrow [\mathbf{VIc}]^{\neq} \longrightarrow CH_2{=}C{=}N\text{–}O\text{–}OH\rceil^{+\cdot}, \quad (23)$$

$$C_2H_3NO_2\rceil^{+\cdot} \rightarrow [\mathbf{Vc}]^{\neq} \longrightarrow CH\text{–}NO\text{–}OH\rceil^{+\cdot}, \quad (24)$$

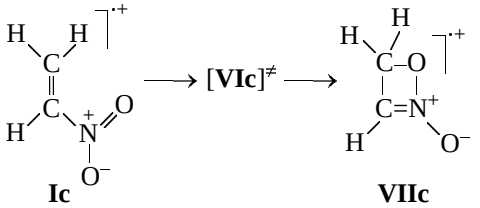

(25)

Examination of the geometric structure of radical cation of **I** revealed existence of two different confor-

Table 2. Dipole moments (μ, D) of 4*H*-1,2-oxazete 2-oxide **VII** and of transition state [**VIII**]$^{\neq}$ and product **VIII** of reaction (13)

Structure	*x*	*y*	*z*	Total
VII	–0.4278	1.1223	1.7739	2.1423
[**VIII**]$^{\neq}$	–3.0836	2.2514	0.0020	3.8180
VIII	1.5675	2.9911	0.0003	3.3770

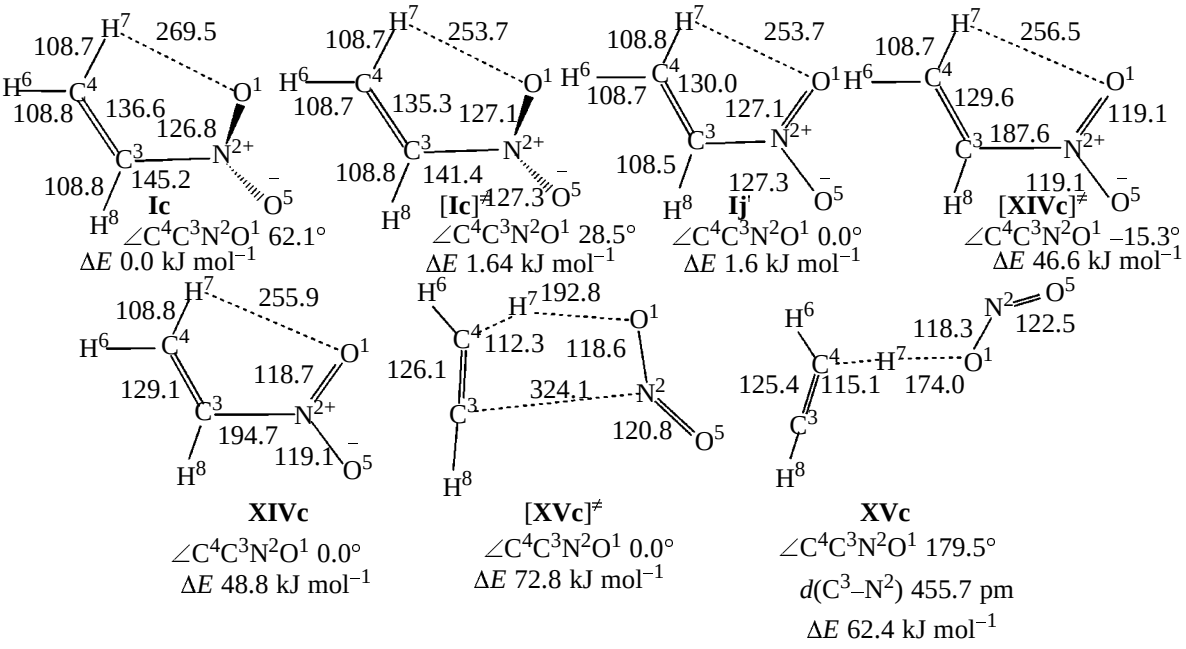

Fig. 8. Geometric parameters of the structures and relative energies of intermediates and transition states between them for cleavage of the C–N bond (**Ic**' → [**Ic**]$^{\neq}$ → **Ic** → [**XIVc**]$^{\neq}$ → **XIVc** → [**XVc**]$^{\neq}$ → **XVc**) in nitroethylene radical cation (bond lengths in pm).

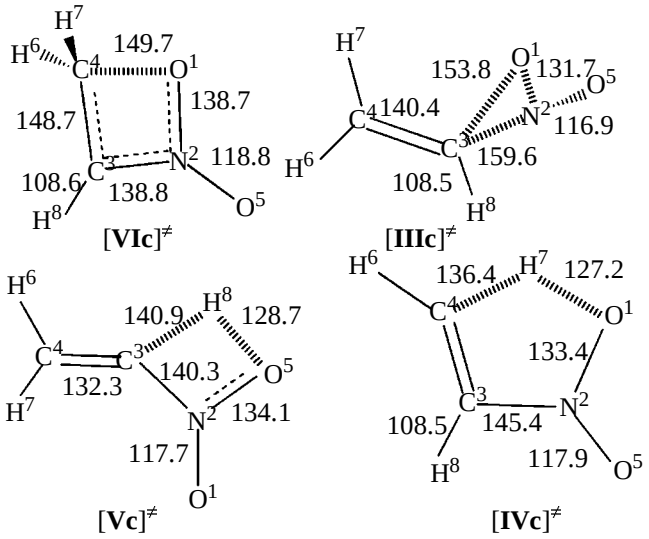

Fig. 9. Structures of the transition states in primary steps of fragmentation of nitroethylene radical cation (cyclization, [**VIc**]$^{\neq}$; nitro–nitrite rearrangement, [**IIIc**]$^{\neq}$; 1,3-H shift, [**Vc**]$^{\neq}$; 1,4-H shift, [**IVc**]$^{\neq}$; bond lengths in pm).

mations: that with the $C^4C^3N^2O^1$ dihedral angle of ~60° (Fig. 8, structure **Ic**; its energy is taken as zero) and a planar conformation (Fig. 9, structure **Ic**', relative energy 1.6 kJ mol^{-1}). Although structures **Ic** and **Ic**' only slightly differ in energy, the corresponding decomposition pathways are essentially different. Radical cation **Ic**' undergoes transformations involving intramolecular hydrogen transfer, whereas species **Ic** undergoes rearrangements (22) and (25). There is a transition state between **Ic** and **Ic**' (Fig. 8, structure [**Ic**]$^{\neq}$), with a barrier of 1.64 kJ mol^{-1} (Fig. 8).

Preliminary study of process (20) shows that the most favorable pathway is cleavage of the C–N bond with formation of the $C_2H_3^+$ cation and $NO_2^{\cdot}$ radical (relative energy 96.5 kJ mol^{-1}). With the positive charge localized on the nitro group, the relative energy is as high as 222.7 kJ mol^{-1}.

A study of the energy variation with stretching of the C–N bond in radical cation of **I** revealed several well-defined transition states and minima (Fig. 8).

The barrier of the reverse reaction **XIVc** → [**XIVc**]$^{\neq}$ → **Ic** is very low, 0.3 kJ mol^{-1} [B3LYP/6-31G(d), without correction for zero-point vibration energy]. With the zero-point vibration energy taken into account, the energy of the intermediate increases to a greater extent (by 2.5 kJ mol^{-1}) than that of the transition state [**XIVc**]$^{\neq}$, since in the transition state the vibration mode with an imaginary frequency corresponds to translation along the reaction coordinate and is therefore excluded from calculation of the zero-point vibration energy. The geometry of **XVc** suggests two possible pathways of further fragmentation, with elimination of the NO_2 group or HNO_2 molecule.

Table 3. Relative energies [B3LYP/6-31G(d), kJ mol^{-1}] of the transition states of reactions involved in monomolecular transformations of nitroethylene radical cation (the energy of nonplanar radical cation **Ic** is taken as zero)

Process	Reaction no.	Compound	$\Delta E_{0\,K}$	$\Delta H_{298\,K}$
C–N bond cleavage	(20)	$C_2H_3NO_2(+,\cdot)$	93.3	96.5
HNO_2 elimination	(21)	$C_2H_3NO_2(+,\cdot)$	–	–
Nitro–nitrite rearrangement	(22)	$C_2H_3NO_2(+,\cdot)$	59.5	58.4
1,3-H shift to *aci* form	(23)	$C_2H_3NO_2(+,\cdot)$	158.7	158.0
1,4-H shift to *aci* form	(24)	$C_2H_3NO_2(+,\cdot)$	96.0	94.1
Cyclization	(25)	$C_2H_3NO_2(+,\cdot)$	54.1	51.8

The results show that the cleavage of the C–N bond in the radical cation is not a barrier-free reaction but occurs by a complex mechanism involving several stable intermediates.

We found that elimination of HNO_2 from the nitroethylene radical cation is not a primary step but can occur as a secondary process within mechanism (24). On the contrary, the barrier of the nitro–nitrite rearrangement (58.4 kJ mol^{-1}) is considerably lower than the dissociation energy of the C–N bond (Table 3, Fig. 9).

For the neutral molecule of **I**, we considered above two alternative routes to the *aci* form and found that the barriers of these reactions are so high that their occurrence as alternative pathways of gas-phase monomolecular decomposition is improbable (Table 1) [31]. However, the barrier of reaction (4) is considerably lower than the activation enthalpy of process (5). For the radical cations, the activation enthalpy of 1,3-H transfer (158.0 kJ mol^{-1}) is considerably higher than the barriers of all the processes considered previously. Therefore, this process is improbable. On the contrary, 1,4-sigmatropic hydrogen shift (relative energy of transition 94.1 kJ mol^{-1}) can under certain conditions compete with the other processes (Table 3, Fig. 9).

As already noted, *ab initio* calculations by various methods and a mass-spectrometric study of monomolecular decomposition of nitroethylene show that only the mechanism of decomposition via 4*H*-1,2-oxazete 2-oxide [reaction (6)] accounts for formation of the detected products. Our study of fragmentation of radical cation of **I** by this mechanism shows that the reaction barrier (51.8 kJ mol^{-1}) is considerably lower than the barriers of all the alternative processes (Table 3). Only the nitro–nitrite rearrangement, with the barrier exceeding that of the cyclization by only 6 kJ mol^{-1}, can make a significant contribution. This conclusion is confirmed by the presence of the peak with m/z 30 in the mass spectra of nitroethylene [33].

Scheme 2 shows the examined pathways of gas-phase monomolecular transformations of radical cation of **I**, including certain secondary processes [B3LYP/6-31G(d)]. The figures at structures are relative enthalpies of formation of the species, and the figures above arrows are relative reaction barriers, kJ mol^{-1} (with the enthalpy of formation of nonplanar nitroethylene radical cation **Ic** taken as zero). A specific feature of radical cations is that they undergo fragmentation difficultly, tending to form various complexes. Therefore, apparently, in many cases we failed to substantiate theoretically the experimentally detected reaction products. We revealed stable intermediates with interatomic distances of 300 pm and more.

Thus, the barriers of reactions involving charged species are considerably lower than the calculated activation enthalpies of decomposition of **I** in the molecular form. Therefore, mass-spectrometric data without additional theoretical studies do not allow unambiguous choice of one or another mechanism of gas-phase decomposition but can be only the starting point for further studies [34].

Mechanism of bimolecular decomposition of nitroethylene. The mechanism of bimolecular decomposition of nitroethylene, which was not studied previously, is of considerable interest. Apparently, the number of possible alternatives in this case is considerably larger than in the monomolecular decomposition.

The B3LYP/6-31G(d) calculation followed the procedure described above. In our study, along with the GAUSSIAN 98 program package [15], we used JAGUAR 4.1 [35].

We found [32] that two nitroethylene (**I**) molecules at certain mutual orientation enter into [2+4] cycloaddition similar to the Diels–Alder reaction. Scheme 3 shows the primary step of the mechanism of bimolecular decomposition of nitroethylene, with the reaction barriers (above arrows) and relative enthalpies of formation of the species, kJ mol^{-1}. Depending on possible orientation of the reactant molecules, we found

Scheme 2.

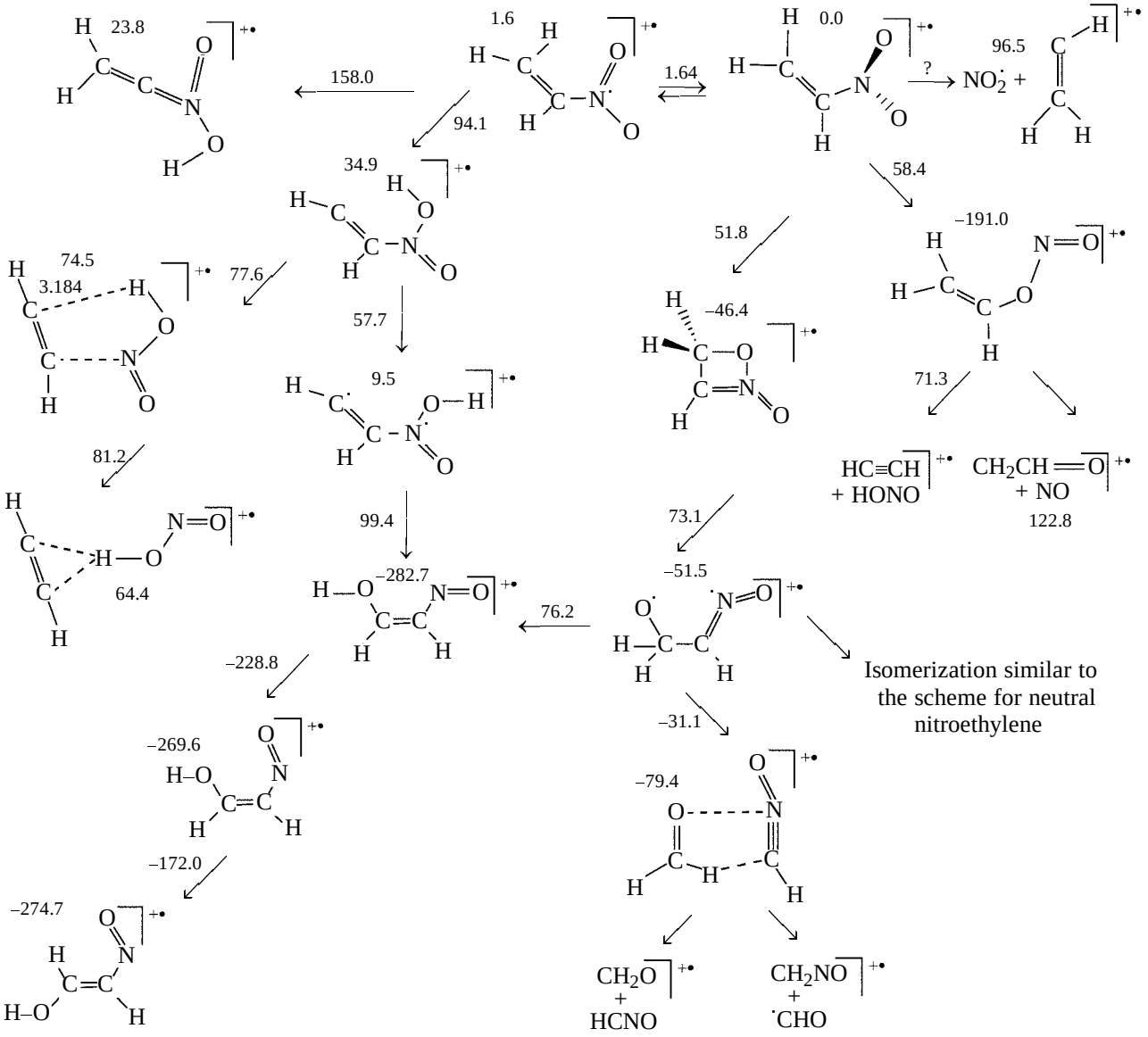

four different transition states and the corresponding products. The products have boat conformations, and the pathways leading to the most stable isomers have high activation enthalpy [steps (26) and (27), Scheme 3].

A study of the further process showed that, e.g., isomer **XVII** (for structure, see Fig. 10) can decompose by two pathways (Scheme 4, with the relative energies given at structures and reaction barriers, at arrows; values in kJ mol^{-1}). The first pathway involves isomerization (28) into compound **XX** with the half-chair conformation, followed by formation of a five-membered ring [**XXII**, reaction (30)], nitro–nitrite rearrangement [**XXIII**, reaction (31)], and elimination of HNO_2 [reaction (32)]. The second pathway via biradical **XXI** is more energetically favorable according to the available data.

The subsequent process involves decomposition of biradical **XXI**; we found that, if the biradical process occurs via step (28) (Scheme 4), the barrier to cleavage of the N–O bond in the ring is 40.5 [reaction (28)] or 41.5 kJ mol^{-1} [reaction (29a)]. The subsequent transformations, after several isomerization steps without significant energy consumption, can yield formaldehyde, nitrile oxide, and nitroethylene (**XXX** or **XXXI**). The molecule of **I** is thus restored, i.e., an autocatalytic cycle is realized.

Scheme 3.

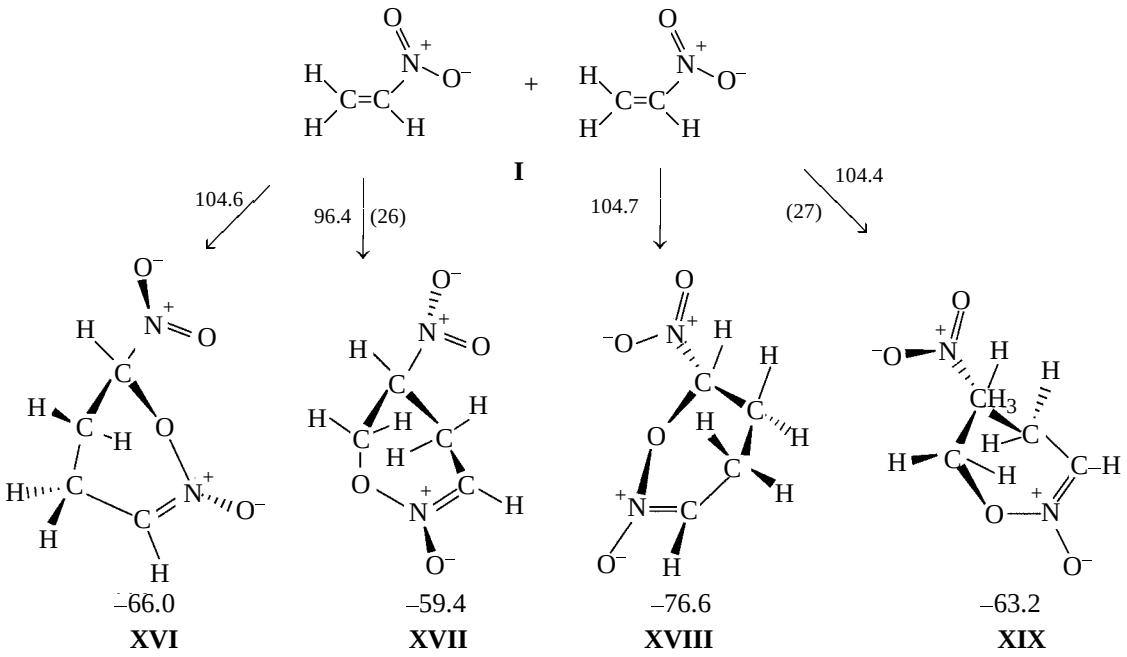

We will not consider in detail the decomposition of **XVI**, **XVII**I, and **XIX**; we will only note that isomer **XVIII** (Scheme 3) can undergo a rearrangement with formation of a five-membered ring (cleavage of the N–O bond in the ring and closure of a new ring through the C–O bond), similar to reaction (30) in Scheme 4; the relative enthalpy of the corresponding transition state is 78.1 kJ mol^{-1}.

Our calculations show that the barriers of the limiting steps of bimolecular decomposition of nitroethylene decrease by a factor of approximately 2 as compared to the corresponding monomolecular processes.

Another interesting conclusion following from the results of this and previous [31, 32] studies is that we revealed a new, relatively general mechanism of decomposition of compounds containing double bonds, involving isomerization into less stable rings and their subsequent decomposition via various biradical struc-

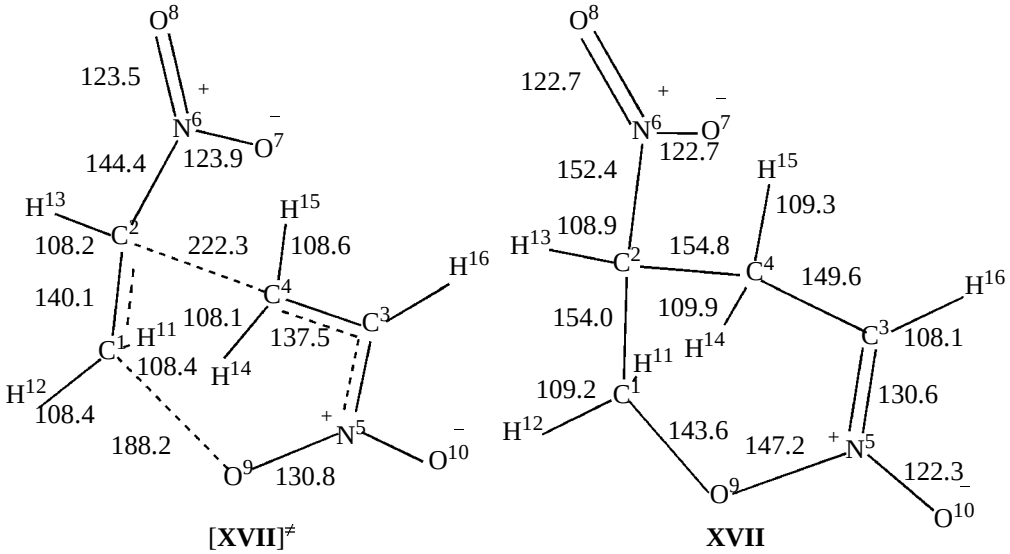

Fig. 10. Geometric parameters of product **XVII** and transition state [**XVII**]$^{\neq}$ of its formation (bond lengths in pm).

Scheme 4.

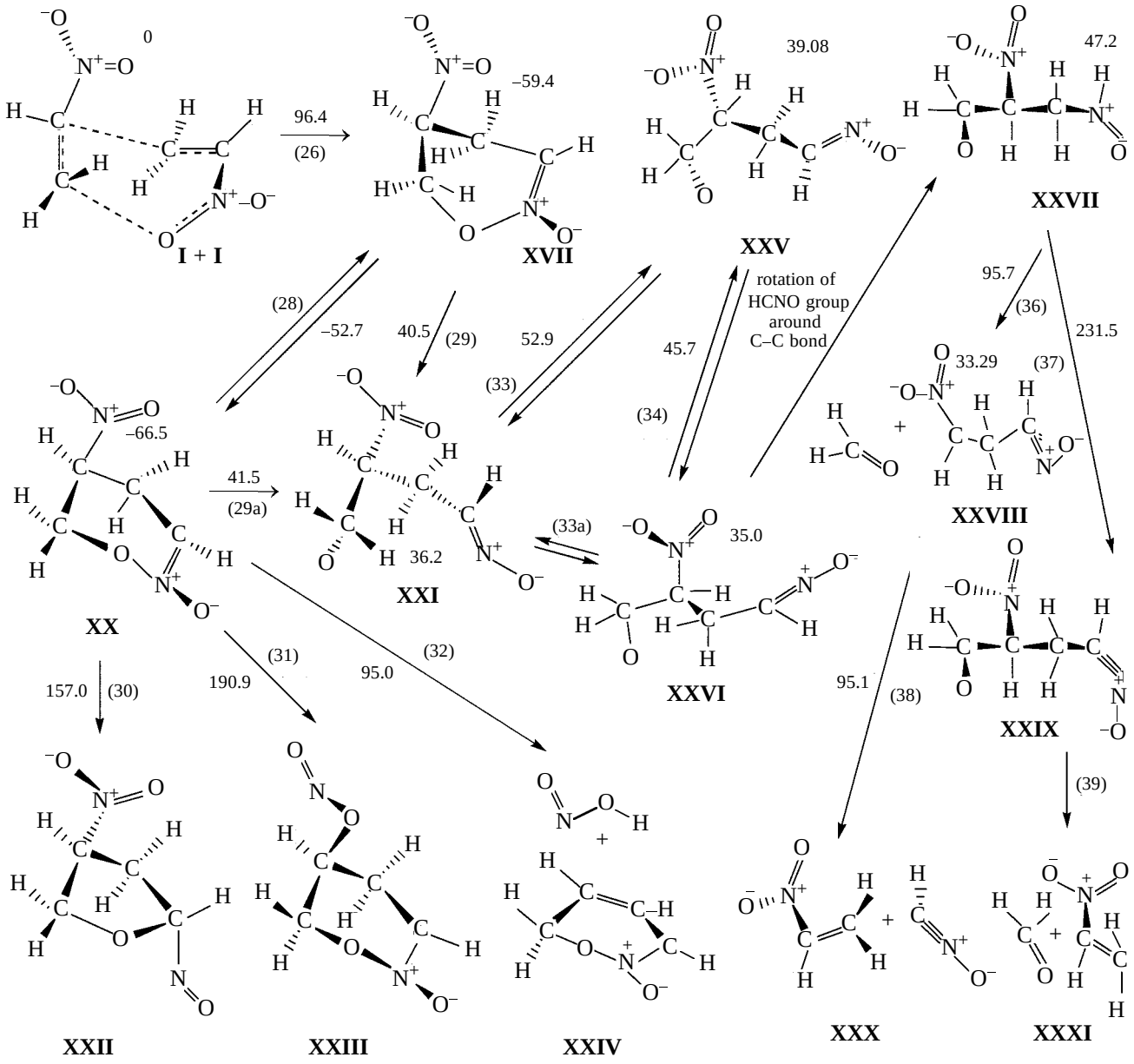

tures. In our papers we considered only one of the possible cyclization pathways, but, apparently, a similar mechanism can be realized in other cyclizations, e.g., in Diels–Alder reactions, 1,3-dipolar cycloadditions, etc.

Thus, a quantum-chemical study shows that the bimolecular pathway of nitroethylene decomposition involves considerably smaller energy consumption compared to monomolecular processes and can be autocatalytic. Apparently, this pathway is improbable in the gas phase at low pressures. However, in the liquid phase and in the gas phase at high pressures the contribution of this process may become significant.

ACKNOWLEDGMENTS

The study was financially supported by the Competition Center for Basic Natural Science, Ministry of Education of the Russian Federation (project no. E00-5.0-311).

REFERENCES

1. Nazin, G.M., Manelis, G.B., and Dubovitskii, D.F., *Usp. Khim.,* 1968, vol. 37, no. 8, p. 1443.
2. Nazin, G.M. and Manelis, G.B., *Usp. Khim.,* 1994, vol. 63, no. 4, p. 327.
3. Manelis, G.B., Nazin, G.M., Rubtsov, Yu.I., and

Strunin, V.A., *Termicheskoe razlozhenie i gorenie vzryvchatykh veshchestv i porokhov* (Thermal Decomposition and Combustion of Explosives and Gunpowders), Moscow: Nauka, 1996. 223 s.

4. Khrapkovskii, G.M., Marchenko, G.N., and Shamov, A.G., *Vliyanie molekulyarnoi struktury na kineticheskie parametry monomolekulyarnogo raspada C- i O-nitrosoedinenii* (Influence of Molecular Structure on Kinetic Parameters of Monomolecular Decomposition of C- and O-Nitro Compounds), Kazan: FEN, 1997.
5. Dubikhin, V.V. and Nazin, G.M., *Izv. Akad. Nauk SSSR, Ser. Khim.*, 1974, no. 4, p. 923.
6. Faustov, V.I., Shevelev, S.A., Anikin, N.A., and Yufit, S.S., *Izv. Akad. Nauk SSSR, Ser. Khim.*, 1979, no. 11, p. 2800.
7. Shamov, A.G., Khrapkovskii, G.M., and Shamov, G.A., in *Struktura i dinamika molekulyarnykh sistem* (Structure and Dynamics of Molecular Systems), Ioshkar-Ola, 1998, issue 5, p. 85.
8. Khrapkovskii, G.M., Shamov, A.G., Shamov, G.A., and Shlyapochnikov, V.A., *Zh. Org. Khim.*, 1999, vol. 35, no. 6, p. 891.
9. Politzer, P., Concha, M.C., Grice, M.E., Murray, J.S., Lane, P., and Habibollazadeh, D., *J. Mol. Struct. (THEOCHEM)*, 1998, vol. 452, no. 10, p. 75.
10. Gindulyte, A., Massa, L., Huang, L., and Karle, J., *J. Phys. Chem. A*, 1999, vol. 103, no. 50, p. 11040.
11. Shamov, A.G. and Khrapkovskii, G.M., in *Struktura i dinamika molekulyarnykh sistem* (Structure and Dynamics of Molecular Systems), Kazan, 1999, issue 6, p. 347.
12. Shamov, A.G. and Khrapkovskii, G.M., in *Struktura i dinamika molekulyarnykh sistem* (Structure and Dynamics of Molecular Systems), Kazan, 1999, issue 6, p. 351.
13. Frisch, M.J., Trucks, G.W., Schlegel, H.B., Gill, P.M.W., Johnson, B.G., Robb, M.A., Cheeseman, J.R., Keith, T.A., Petersson, G.A., Montgomery, J.A., Raghavachari, K., Al-Laham, M.A., Zakrzewski, V.G., Ortiz, J.V., Foresman, J.B., Cioslowski, J., Stefanov, B.B., Nanayakkara, A., Challacombe, M., Peng, C.Y., Ayala, P.Y., Chen, W., Wong, M.W., Andres, J.L., Replogle, E.S., Gomperts, R., Martin, R.L., Fox, D.J., Binkley, J.S., Defrees, D.J., Baker, J., Stewart, J.P., Head-Gordon, M., Gonzalez, C., and Pople, J.A., *GAUSSIAN 94*, Pittsburgh: Gaussian, 1995.
14. Becke, A.D., *J. Chem. Phys.*, 1993, vol. 98, no. 2, p. 1372.
15. Frisch, M.J., Trucks, G.W., Schlegel, H.B., Scuseria, G.E., Robb, M.A., Cheeseman, J.R., Zakrzewski, V.G., Montgomery, J.A., Stratmann R.E., Burant, J.C., Dapprich, S., Millam, J.M., Daniels, A.D., Kudin, K.N., Strain, M.C., Farkas, O., Tomasi, J., Barone, V., Cossi, M., Cammi, R., Mennucci, B., Pomelli, C., Adamo, C., Clifford, S., Ochterski, J., Petersson, G.A., Ayala, P.Y., Cui, Q., Morokuma, K., Malick, D.K., Rabuck, A.D., Raghavachari, K., Foresman, J.B., Cioslowski, J., Ortiz, J.V., Stefanov, B.B., Liu, G., Liashenko, A., Piskorz, P., Komaromi, I., Gomperts, R., Martin, R.L., Fox, D.J., Keith, T., Al-Laham, M.A., Peng, C.Y., Nanayakkara, A., Gonzalez, C., Challacombe, M., Gill, P.M.W., Johnson, B.G., Chen, W., Wong, M.W., Andres, J.L., Head-Gordon, M., Replogle, E.S., and Pople, J.A., *GAUSSIAN 98*, Rev. A.1, Pittsburgh: Gaussian, 1998.
16. Stewart, J.J.P., *J. Comput. Chem.*, 1989, vol. 10, no. 209, p. 221.
17. Peng, C. and Schlegel, H.B., *Israel J. Chem.*, 1993, vol. 33, p. 449.
18. Baker, J., *J. Comput. Chem.*, 1986, vol. 7, no. 4, p. 385.
19. Foresman, J.B. and Frisch, A., *Exploring Chemistry with Electronic Structure Methods*, Pittsburgh: Gaussian, 1996, p. 188.
20. Khrapkovskii, G.M., Chachkov, D.V., and Shamov, A.G., in *Struktura i dinamika molekulyarnykh sistem* (Structure and Dynamics of Molecular Systems), Kazan, 1999, issue 6, p. 358.
21. Dubikhin, V.V., Nazin, G.M., and Manelis, G.B., *Izv. Akad. Nauk SSSR, Ser. Khim.*, 1974, no. 6, p. 1345.
22. Khrapkovskii, G.M., Shamov, A.G., and Shamov, G.A., in *Svoistva veshchestv i stroenie molekul* (Properties of Substances and Molecular Structure), Tver: Tversk. Gos. Univ., 1998, p. 41.
23. Dewar, M.J.S., Ritchie, J.P., and Alster, J., *J. Org. Chem.*, 1985, vol. 50, no. 7, p. 1031.
24. Khrapkovskii, G.M., Shamov, A.G., Shamov, G.A., and Slyapochnikov, V.A., *Mendeleev Commun.*, 1997, no. 5, p. 169.
25. Khrapkovskii, G.M., Nikolaeva, E.V., Chachkov, D.V., and Shamov, A.G., *Zh. Obshch. Khim.*, 2004, vol. 74, no. 6, p. 983.
26. Gurvich, L.V., Karachevtsev, G.V., Kondrat'ev, V.N., Lebedev, Yu.A., Medvedev, V.A., Potapov, V.K., and Khodeev, Yu.S., *Energiya razryva khimicheskikh svyazei. Potentsialy ionizatsii i srodstvo k elektronu* (Dissociation Energies of Chemical Bonds. Ionization Potentials and Electron Affinities), Moscow: Nauka, 1974.
27. Khrapkovskii, G.M., Shamov, A.G., Shamov, G.A., Nikolaeva, E.V., and Chachkov, D.V., *Khim. Komp'yut. Model., Butlerovsk. Soobshch.*, 2002, no. 6, p. 17.

28. Kinstle, T.H. and Stam, J.G., *J. Org. Chem.*, 1970, vol. 35, no. 6, p. 1771.

29. Wiser, K. and Berndt, A., *Angew. Chem.*, 1975, vol. 87, no. 2, p. 72.

30. Wiser, K. and Berndt, A., *Angew. Chem.*, 1975, vol. 87, no. 2, p. 73.

31. Shamov, A.G. and Khrapkovskii, G.M., *Mendeleev Commun.*, 2001, no. 4, p. 163.

32. Shamov, A.G., Nikolaeva, E.V., and Khrapkovskii, G.M., in *Struktura i dinamika molekulyarnykh sistem* (Structure and Dynamics of Molecular Systems), Kazan, 2002, issue 9, part 2, p. 277.

33. Egsgaard, H. and Carlsen, L., *Org. Mass Spectrom.*, 1989, vol. 24, no. 9, p. 1031.

34. Nikolaeva, E.V., Shamov, A.G., and Khrapkovskii, G.M., in *Struktura i dinamika molekulyarnykh sistem* (Structure and Dynamics of Molecular Systems), Ioshkar-Ola, 2001, issue 8, part 2, p. 190.

35. *JAGUAR 4.1*, Portland: Schrödinger, 2000.